Reversible metamorphosis in a bacterium

Karina Ramijan[1], Joost Willemse[1], Eveline Ultee[1], A. Joeri Wondergem[2], Anne van der Meij[1], Ariane Briegel[1], Doris Heinrich[2], Gilles P. van Wezel[1], and Dennis Claessen[1,#]

[1] Molecular Biotechnology, Institute Biology Leiden, Leiden University. [2] Leiden Institute of Physics (LION), Huygens-Kamerlingh Onnes Laboratory. Leiden University.

To whom correspondence should be addressed:

E-mail: D.Claessen@biology.leidenuniv.nl

Tel: +31 (0)71 527 5052

Keywords: reversible metamorphosis, cell wall synthesis, cell division, origin of life, L-forms, synthetic biology

ABSTRACT

The cell wall is a shape-defining and protective structure that envelops virtually all bacteria. Wall-less variants, called L-forms, have been generated in laboratories for many decades under highly specialized conditions, invariably aimed at interrupting cell wall synthesis. As such, the relevance of these cells has remained obscure. Here we show that the filamentous actinomycete *Kitasatospora viridifaciens* has the natural ability to switch between a wall-less state and the canonical mycelial mode-of-growth. We show that this organism thrives in a cell wall-less form, and identify the polar growth determinant DivIVA as an essential regulator required for reversible metamorphosis. This is the first report of a reversible metamorphosis in a bacterium that includes wall-less cells as a natural stage in bacterial development.

INTRODUCTION

The cell wall, an essential component of virtually all bacteria, is a dynamic structure that largely determines bacterial cell shape[1]. It provides structural rigidity and protection to osmotic stresses and forms the barrier between the bacterium and its environment[2,3]. Given its protective role, the cell wall and its biosynthetic enzymes are targets of some of the best known antibiotics, including penicillin and vancomycin[4,5]. The synthesis of its major constituent, peptidoglycan (PG), involves the activity of large protein complexes that cooperatively build and incorporate new PG precursors into the growing glycan strands at the cell surface[3,6,7]. These strands are then cross-linked to form in essence a single, giant sacculus[8]. Major differences in growth and cell division are seen between the planktonic firmicutes that grow via lateral cell-wall growth, and the Actinobacteria, which include many multicellular genera that form complex mycelia and grow via apical extension[9,10]. A large number of genes required for PG synthesis and cell division are organized in the highly conserved *dcw* gene cluster (for division and cell wall synthesis), which contains the cell division scaffold FtsZ[11,12]. Some genes in this cluster have gained species-specific functions, or have been lost during evolution. A well-known example is DivIVA: in *Bacillus subtilis,* this protein is involved in septum-site localization by preventing accumulation of the cell division initiator protein FtsZ[13]. In contrast, in filamentous actinomycetes, DivIVA is a crucial component of the polarisome complex that drives polar growth[14,15]. As a consequence, *divIVA* is dispensable in *B. subtilis* but essential in actinomycetes[14,16]. Conversely, cell division is not essential for growth in streptomycetes, and uniquely, *ftsZ* and various other genes that encode members of the divisome can be deleted[17,18]. These examples imply a major evolutionary diversification that has separated Actinobacteria from other bacteria.

Although the cell wall is a vital structure for bacteria, several species can be manipulated to produce cells that propagate without their wall, which are known as L-forms[19-22]. Typically, this was done in an artificial way, by growing strains on osmo-protective media in the presence of high levels of antibiotics targeting the enzymes required for cell-wall synthesis[23-25]. More recently, L-form growth was also achieved genetically by turning off PG synthesis[20,26]. These approaches often yield unstable L-form variants that quickly revert to the walled state when the inducing agents are omitted. By contrast, stable L-forms can propagate indefinitely without the cell wall and require two kinds of mutations[27]. The first class of mutations leads to an increase in membrane synthesis, either directly by increasing fatty acid biosynthesis, or indirectly by reducing cell wall synthesis[28]. The second class of mutations reduces oxidative damage caused by reactive oxygen species, which are detrimental to formation of L-forms[29]. Notably, proliferation of L-forms is independent of the FtsZ-based division machinery[20,30]. Instead, their proliferation can be explained solely by biophysical processes, in which an imbalance in the cell surface area to volume ratio leads to spontaneous blebbing and the generation of progeny cells[28]. This purely biophysical mechanism of L-form proliferation is independent of the prokaryotic lineage. This observation has led to the hypothesis that early life forms propagated in a similar fashion well before the cell wall had evolved[20,28,31]. Until now, no examples are known of bacteria that generate L-form cells in the absence of the commonly used inhibitors of cell-wall synthesis and that propagate without accumulating mutations.

Here we present evidence that filamentous actinomycetes have the natural ability to form such wall-less cells. These cells can propagate in the wall-less state, but can also revert to mycelial growth. Our work provides the first direct evidence that L-form cells are a natural stage in bacterial life.

Transitions between filamentous and L-form growth

One of the key requirements for growth of L-form cells is the presence of an osmotically balanced medium to prevent cell lysis. Unexpectedly, when the actinomycete *Kitasatospora viridifaciens* (previously called *Streptomyces viridifaciens*[32]) is grown in liquid LPB (containing high levels of sucrose) in the absence of any cell wall synthesis inhibitor, spherical vesicles were visible at low frequency in the culture broth and in between the mycelial networks (Fig. 1A). Replacing sucrose by an equimolar amount of NaCl also leads to the formation of such vesicles, although they are less abundant and smaller than those formed in LPMA containing sucrose (Extended Data Fig. S1B). In the absence of either osmolyte, we could not detect any vesicles (Extended Data Fig. S1C). The spherical vesicles often contained smaller vesicles inside and are surrounded by a membrane. Importantly, staining with SYTO9 indicated that these vesicles contained DNA (Fig. 1B), while transmission EM indicated that they contained no cell wall (Fig. 1C, D), which make them very reminiscent of L-form-like cells. Comparable DNA-containing vesicles were also observed during growth of *Kitasatospora* strains MBT63 and MBT66[32], as well as *Streptomyces venezuelae*. However, they were not detected in *Streptomyces coelicolor*, *Streptomyces griseus* or in *Streptomyces lividans* (Extended Data Fig. S2).

To determine the location where these L-form-like cells originate from in the context of the hyphae, we performed live imaging of growing colonies (Fig. 1E; Extended Data Video S1). Approximately 7 hr after the visible emergence of germ tubes, we detected a transient arrest in tip extension of the leading hypha (Fig. 1E, t=430 mins). By that time, L-form-like cells became visible, which were extruded from the hyphal tip (see arrow in Fig. 1E). After the extrusion process, the leading

hypha resumed elongation. Subapically, new branches became visible about 210 minutes after the first appearance of these cells (Extended Data Video S1, t= 640 min). Notably, such branches frequently also extruded L-form-like cells, similarly to the leading hypha (Extended Data Video S2). This showed that the L-form-like cells are produced at hyphal tips.

To study the viability of these L-form-like cells, we separated them from the mycelia by filtration, and used the filtrate to inoculate fresh LPB medium. Strikingly, these cells were able to proliferate in a manner reminiscent of the extrusion-resolution mechanism that was previously described for proliferation of *B. subtilis* L-forms[20] (Fig. 1F; Extended Data Video S3). Apparently, these wall-less cells are natural L-forms that can proliferate without the need for any genetic mutations. To discriminate these natural L-forms from other stable and unstable L-forms generated by inducing agents, we hereinafter refer to them as N-forms (for natural L-forms).

When N-forms were plated on solid LPMA medium, we noticed that some of the cells generated colonies consisting of both mycelia and N-form cells, implying that these N-forms can revert to mycelial growth (Fig. 1G; Extended Data Video S4). To exclude that mycelial growth was caused by outgrowing spores present in the filtrate, we also analysed a non-sporulating Δ*ssgB* mutant of *K. viridifaciens* (Extended Data Fig. S3A-C). Like the wild-type strain, the N-forms of the Δ*ssgB* mutant propagated in the wall-less state in liquid, and reverted to mycelial growth on solid medium (Extended Data Fig. S3D, E; Extended Data Video S5).

Altogether, this work thus presents the first example of a bacterium with the natural ability to generate wall-less cells as a natural stage in bacterial life. These cells can propagate without their cell wall, but can also revert to mycelial growth (Fig. 1H).

Generation of the stable L-form lineage *alpha*

Although N-forms could propagate in the wall-less state, their phenotype was reversible leading to mixtures of both hyphae and N-forms. To understand the mechanism of this reversible metamorphosis, we aimed to generate a strain that could reproducibly switch between an all-walled and completely wall-less state. To this end, we exposed the wild-type strain to penicillin and lysozyme following a weekly sub-culturing regime to obtain a derivative strain, which we designated *alpha*. As intended, in sucrose-based media *alpha* exclusively proliferated in the L-form-like state and showed no signs of reversion (Fig. 2A; Extended Data Video S6). Characterization using transmission electron microscopy (TEM) confirmed that *alpha* contained no PG-based cell wall (Fig. 2B). Excitingly, while *alpha* cells preferred the L-form state, they still possessed the capacity of reversible metamorphosis. When *alpha* was streaked onto plates lacking osmotic protectants, mycelial colonies were obtained (Fig. 2C). Conversely, when mycelial colonies were transferred to plates containing sucrose, the formation of L-form cells was readily induced, which, like in the parental wild-type strain, emerged from the hyphal tip (Extended Data Video S7). However, unlike the N-forms generated by the wild-type strain, the L-forms formed by *alpha* indefinitely propagated in the wall-less state and did not revert to mycelial growth on osmo-protective media.

To see if we could identify the mutations that predisposed proliferation in the L-form state, we performed SNP analysis by comparing the genome sequence of *alpha* to that of the parent DMS40239[33]. This revealed that *alpha* had lost the 1.7MB linear plasmid KVP1 that is present in the wild-type strain. In addition, three SNPs were identified in the genome (Extended Data Table 1). One of the mutations mapped to a non-coding DNA region between two genes encoding a putative glutamine-

fructose-6-phosphate transaminase and an ABC transporter, respectively. A second mutation was identified in one of the two *lysX* genes (BOQ63_22710), and which encodes a bifunctional phosphatidylglycerol lysyltransferase[34,35]. This protein is involved in lipid modification by transferring L-lysine from lysyl-tRNA to phosphatigylglycerol. This mutation resulted in a T183I mutation in LysX. The third SNP was in *uppP* (BOQ63_21575), resulting in an L58M change in its gene product undecaprenyl-diphosphate phosphatase. This phosphatase is involved in the recycling pathway of the carrier lipid undecaprenyl phosphate, which transports glycan biosynthetic intermediates for cell wall synthesis[36]. While their function related to cell-wall or membrane synthesis is suggestive at least, and they may therefore facilitate proliferation in the L-form state, none of them blocked reversible metamorphosis.

DivIVA is essential for reversible metamorphosis

DivIVA is required for polar growth in *Streptomyces* and *Corynebacteria*[14,16]. We therefore wondered if DivIVA has a role in the formation or proliferation of *K. viridifaciens* L-forms, which lack any obvious polarity. To address this question, we first created plasmid pKR3, which leads to the constitutive expression of a C-terminal eGFP fusion to DivIVA, which was partially active (see below). Analysis of a transformant constitutively expressing DivIVA-eGFP revealed that the chimeric protein localized to hyphal tips (Fig. 2D). This apical localization pattern is consistent with earlier findings in streptomycetes[14]. Notably, some hyphae expressing the fusion protein were wider and showed hyphal tip-splitting, which may be due to a polar effect or deregulated expression of DivIVA. To localize DivIVA in the L-form state, we made use of the fact that the generated strain reverts to the L-form mode-of-

181 growth on osmoprotective media. Despite the absence of polarity, L-forms containing
182 pKR3 typically showed one or two DivIVA foci per cell, which invariably were
183 localized to the membrane (Fig. 2D). In contrast, no foci were detected in L-form
184 cells constitutively expressing eGFP (pGreen) or those containing the empty plasmid
185 (pKR1).

186 We then constructed plasmids pKR4 to delete *divIVA* and pKR5 to delete a
187 large part of the *dcw* gene cluster, which includes *divIVA*[11] (Fig. 3A). Introduction of
188 these plasmids into *alpha* by transformation and subsequent screening yielded the
189 desired *divIVA* and *dcw* mutants. Western blot analysis using antibodies against
190 DivIVA of *Corynebacterium glutamicum* confirmed the absence of DivIVA in both
191 the *divIVA* and the *dcw* mutant (Fig. 3B). Analysis of growth in LPB medium or on
192 solid LPMA plates indicated that the L-form cells proliferated normally in the absence
193 of *divIVA* or part of the *dcw* gene cluster (Fig. 3C, D). However, when L-form cells
194 were plated on MYM medium, only the *alpha* strain could grow due to its ability to
195 form mycelial cells, while the *divIVA* and *dcw* mutants could not grow due to their
196 failure to undergo reversible metamorphosis (Fig. 3D). Introduction of plasmid pKR6
197 containing *sepF-sepG-divIVA* under control of their natural promoters restored growth
198 to the *divIVA* null mutant on MYM medium (Fig. 3D). To exclude that this was
199 caused by the additional *sepF* and *sepG* genes, we also introduced plasmid pKR7,
200 which expresses *divIVA* from the constitutive *gap1* promoter. This plasmid also
201 complemented growth of the *divIVA* mutant on MYM medium, thus establishing that
202 *divIVA* alone was sufficient to complement the *divIVA* null mutant (Fig. 3D).
203 Importantly, the DivIVA-eGFP fusion protein also restored filamentous growth to the
204 *divIVA* mutant, implying that the chimeric protein is largely functional *in vivo*.
205 However, some hyphae showed apical branching or tip-splitting indicative of polar

effects on growth and development (Extended Data Fig. S4). Altogether, these results identify DivIVA as a key protein that is essential for reversible metamorphosis.

Functional complementation of the *K. viridifaciens dcw* mutant by the *S. coelicolor dcw* gene cluster

The unique capacity of *alpha* to switch back-and-forth between a walled, filamentous mode-of-growth and a wall-less L-form state provides a unique platform to apply an engineering approach to cell morphology design. As a first step towards that goal, we introduced the *dcw* gene cluster from *S. coelicolor* into the *K. viridifaciens dcw* mutant (Fig. 3D, E). Excitingly, introduction of this gene cluster restored filamentous growth and reversible metamorphosis (Fig. 3D, E), demonstrating that the *S. coelicolor dcw* cluster functionally replaces the *dcw* cluster of *K. viridifaciens*. This is an important observation as it also shows that the ability of *K. viridifaciens* to undergo reversible metamorphosis is not dictated by specific adaptation in this organism of genes within its *dcw* cluster. Staining of nascent PG synthesis by fluorescent vancomycin (Van-FL) revealed a ladder-like staining pattern in the complemented *dcw* mutant, which could not be discriminated from that observed for the *alpha* strain growing as a mycelium (Fig. 3E). These ladders represent sites where PG-based septa are formed in an FtsZ-dependent manner[37]. Altogether, this demonstrates that the mycelium formed by this 'hybrid' bacterium is established by the activity of the macromolecular machinery of two different bacteria belonging to separate genera. This paves the way for extending this principle with *dcw* gene clusters of morphologically distinct bacteria, such as the unicellular actinobacteria *Corynebacterium glutamicum* and *Mycobacterium tuberculosis*.

DISCUSSION

Filamentous actinomycetes have been studied for more than 50 years as a model for multicellular bacterial development. We here provide compelling evidence that the formation of wall-less cells is a natural, and previously unnoticed developmental stage in these organisms. These natural wall-less cells, which we have dubbed N-forms, are extruded from the hyphal tips, contain DNA and are viable as concluded from their ability to form colonies. This work thus presents the first example of a bacterium with the natural ability to generate wall-less cells and provides a major step in our ability to reveal the ecological relevance of these enigmatic wall-less cells. It will be of key interest to dissect how this unique morphogenetic switch is regulated and to disclose how widespread this phenomenon is.

The spontaneous release of N-forms provides an important step forward towards characterising where such cells are found in nature. Actinomycetes are abundantly present in soil and marine environments and are known to interact with many eukaryotic organisms, such as insects and plants[38,39]. Interestingly, the phloem of plants is rich in sucrose and provides a supportive environment to sustain wall-less cells[40,41]. Given their presence in soil environments, we envision that these actinomycetes may associate with plant roots in their filamentous state, followed by a switch to the wall-less state allowing them to quickly travel throughout the plant tissue or via the phloem. In this way, they may be able to traverse long distances to the sites where their activity is required, for instance in providing protection to the plant mediated by their large repertoire of secondary metabolites they produce[38,42]. However, for other species this transient mode-of-growth, during which the wall-less cells may escape from the plant immune system, could also help to cause damage to plants. In this context it is interesting to note that we have been able to induce L-form

256 growth in the potato pathogen *Streptomyces scabies*, which, as a non-sporulating
257 strain, is known to traverse long distances within the plant (R. Loria, personal
258 communication). More generally, we suppose that wall-less cells may be more
259 commonly present in nature, but have simply been overlooked due to their specific
260 requirements for growth.

261 N-forms are released from hyphal tips, which contain extended membrane
262 structures[37]. One of the key requirements for L-form proliferation is an upregulation
263 of membrane synthesis[28]. We think that the presence of these extended membranes at
264 the hyphal tip may facilitate the formation of N-forms in these actinomycetes. Their
265 release from the hyphal tip coincides with an arrest in tip extension, indicating that
266 PG synthesis at those sites is transiently blocked. Notably, sequencing of the genome
267 of the stable L-form lineage *alpha* identified two mutations that may exert their effect
268 on PG synthesis. One mutation was identified in the non-coding region of a gene
269 encoding a protein controlling the flux of glucose in the hexosamine pathway,
270 ultimately leading to synthesis of PG precursors. A second mutation was found in
271 *uppP*, which is involved in PG precursor recycling. While these mutations may
272 regulate cell-wall precursor accumulation, none of them was essential for mycelial
273 growth. This can be derived from the fact that both N-forms as well as the L-forms
274 formed by *alpha* may revert to mycelial growth. However, the fact that the mutations
275 do not prevent mycelial growth does not rule out that they may have been essential for
276 the formation of a previous lineage that finally evolved into *alpha*. The role of the
277 mutations and their contribution to the formation of N-forms and proliferation of
278 *alpha* is under current investigation.

279 Summarising, our work on reversible metamorphosis provides the first
280 evidence for the existence of natural wall-less cells, and thereby broadens the large

diversity in bacterial cell shapes[1]. Finally, it will enable us to design 'hybrid' bacteria with dramatically changed cell morphologies by replacing some of the most fundamental shape-defining genes. Ultimately, this should allow us to convert a truly multicellular bacterium into a walled, unicellular derivative, which is not only exciting from an evolutionary point-of-view, but which may also prove valuable as an industrial workhorse for the biosynthesis of natural products. The functional replacement of the *dcw* gene cluster between bacteria from distinct genera provides an important first step towards that goal.

METHODS

Strains and media

Bacterial strains used in this study are shown in Extended Data Table 2. To obtain sporulating cultures, *Streptomyces* and *Kitasatospora* species were grown at 30°C for 4 days on MYM medium, containing (w/v) 0.4% maltose, 0.4% yeast extract, 1% malt extract, 2% Iberian agar,0.2 (v/v) R5 trace elements[43]. To support growth of wall-less cells, strains were grown in liquid L-Phase Broth (LPB), containing (w/v) 0.15% yeast extract, 0.25% bacto-peptone, 0.15% oxoid malt extract, 0.5% glucose, 22% sucrose, 1.5% oxoid tryptone soya broth powder and 25 mM $MgCl_2$. Alternatively, wall-less cells were propagated in liquid L-Phase Medium (LPM), containing (w/v) 0.5% glucose, 0.5% yeast extract, 0.5% peptone, 20% sucrose, 0.01% $MgSO_4 \cdot 7H_2O$, and 25 mM $MgCl_2$. Cultures were inoculated with 10^6 spores ml^{-1} and grown in 250 ml flasks. Cultures were incubated at 30°C, while shaking at 100 rpm. For propagation of wall-less cells on solid medium, we used LPMA (i.e. LPM supplemented with (w/v) 0.75% Iberian agar and 5% (v/v) horse serum).

Generation of the stable *K. viridifaciens* L-form lineage *alpha* was performed in LPB, following the cultivation regime previously described[44]. 50 ml cultures were grown in 250 ml flasks in an orbital shaker at 100 rpm.

For general cloning purposes, *E. coli* strains DH5α and JM109 were used, while *E. coli* ET12567 and SCS110 were used to obtain unmethylated DNA (Extended Data Table 2). *E. coli* strains were grown at 37 °C in LB medium, supplemented with chloramphenicol (25 μg ml^{-1}), ampicillin (100 μg ml^{-1}), apramycin (50 μg ml^{-1}), kanamycin (50 μg ml^{-1}), or viomycin (30 μg ml^{-1}), where necessary.

Construction of plasmids

All plasmids and primers used in this work are shown in Extended Data Table 3 and Extended Data Table 4, respectively.

Construction of the DivIVA localization construct pKR3

To localize DivIVA, we first created plasmid pKR2 containing a viomycin resistance cassette cloned into the unique NheI site of pIJ8630[45]. To this end, the viomycin resistance cassette was amplified from pIJ780[46] with the primers *vph*-FW-NheI and *vph*-RV-NheI. Next, we amplified the strong constitutive *gap1* promoter as a 450 bp fragment from the genome of *S. coelicolor* with the primers P_{Gap1}-FW-BglII and P_{Gap1}-RV-XbaI. We also amplified the *divIVA* coding sequence (the +1 to +1335 region relative to the start codon of *divIVA* (BOQ63_31065) from the chromosome of *K. viridifaciens* using primers *divIVA*-FW-XbaI and *divIVA*-no stop-RV-NdeI. Finally, the promoter and *divIVA* coding sequence were cloned into pKR2 as a BglII/XbaI and XbaI/NdeI fragment respectively, yielding plasmid pKR3.

330 *Construction of the deletion constructs pKR1, pKR4 and pKR5*

331 The *ssgB* mutant was created in *K. viridifaciens* using pKR1, which is a derivative of
332 the unstable plasmid pWHM3[47]. In the *ssgB* mutant, nucleotides +20 to +261 relative
333 to the start codon of *ssgB* were replaced with the *loxP-apra* resistance cassette as
334 described[48]. A similar strategy was used for the deletion of the *divIVA* gene or part of
335 the *dcw* cluster, using plasmids pKR4 and pKR5, respectively. In the *divIVA* deletion
336 mutant, nucleotides +205 to +349 relative to the start codon of *divIVA*
337 (BOQ63_31065) were replaced with the apramycin resistance cassette, whereas in the
338 *dcw* mutant the chromosomal region from +487 bp relative to the start of the *ftsW*
339 gene (BOQ63_31025) until +349 relative to the start of the *divIVA* gene was replaced
340 with the apramycin resistance marker.

341

342 *Construction of the complementation constructs pKR6 and pKR7*

343 The constructs pKR6 and pKR7 were created to complement the *divIVA* mutant. For
344 complementation of *divIVA* under control of its native promoter, the genomic
345 sequence from -1565 to +1357 relative to the translational start site of *divIVA* was
346 amplified from the chromosomal DNA of *K. viridifaciens* using the primers *sepF-*
347 *sepG-divIVA*-FW-BglII and *sepF-sepG-divIVA*-RV-XbaI. This product contained the
348 coding sequences of *sepF*, *sepG* and *divIVA* including the native *divIVA* promoter,
349 and was cloned into the integrative vector pIJ8600[45].

350 The pKR7 plasmid was constructed for the expression of *divIVA* from the
351 constitutive *gap1* promoter. To this end, the promoter region of *gap1* was amplified
352 with the primers P_{gap1}-FW-BglII and P_{gap1}-RV-XbaI using *S. coelicolor* genomic
353 DNA as the template. The *divIVA* coding sequence was amplified from the genome of
354 *K. viridifaciens* with the primers *divIVA*-XbaI-FW and *divIVA*-NdeI-RV. Finally, both

the *gap1* promoter and *divIVA* coding sequence were cloned as BglII/XbaI and XbaI/NdeI fragments into the integrative vector pIJ8600[45]. All constructs were sequenced for verification.

For the orthologous complementation of the *K. viridifaciens dcw* mutant, the *S. coelicolor* cluster from cosmid ST4A10[49] was used. The ST4A10 cosmid was cut with BglII and ScaI, followed by gel extraction of a 13,268 bp BglII fragment, encompassing the partial *S. coelicolor dcw* cluster. This fragment was subsequently ligated into BglII-digested pIJ8600, yielding pKR8.

Filtration of N-forms

An individual colony of *K. viridifaciens* DSM40239 that had been grown on MYM medium for 4 days was used to inoculate 50 ml LPB medium. The culture was grown for 7 days at 30°C in an orbital shaker at 100 rpm. To separate the mycelium from the N-forms, the culture was passed through a sterile filter made from an EcoCloth™ wiper. A subsequent filtration step was done by passing the N-forms through a 5 µm Isopore™ membrane filter. The filtered cells were centrifuged at 1,000 rpm for 40 min, after which the supernatant was carefully removed by decantation to avoid disturbance of the cells.

Transformation of L-forms

Transformation of *alpha* essentially followed the protocol for the rapid small-scale transformation of *Streptomyces* protoplasts[50], with the difference that 50 µl cells from a mid-exponential growing L-form culture were used instead of protoplasts. Typically, 1 µg DNA was used for each transformation. Transformants were selected by applying an overlay containing the required antibiotics in P-buffer after 20 hours.

Further selection of transformants was done on LPMA medium containing the appropriate antibiotics.

Microscopy

Strains grown in LPB or LPMA were imaged using a Zeiss Axio Lab A1 upright microscope equipped with an Axiocam Mrc. A thin layer of LPMA (without horse serum) was applied to the glass slides to immobilize the cells prior to the microscopic analysis.

Fluorescence microscopy

Fluorescence microscopy pictures were obtained with a Zeiss Axioscope A1 upright fluorescence microscope with an Axiocam Mrc5 camera. Live cells were stained with SYTO 9 (0.05 mM) and BODIPY vancomycin (1 μg ml^{-1}) for 10 min to detect DNA and nascent PG, respectively. Stains were obtained from Molecular Probes™. The fluorescent images were obtained using a 470/40 nm band pass excitation and a 505/560 band pass detection, using an 100x N.A. 1.3 objective. Stained live cells where immobilized on microscope slides using a thin layer of LPMA (without horse serum). To obtain a sufficiently dark background, the background of the images was set to black. These corrections were made using Adobe Photoshop CS5.

Time-lapse microscopy

For visualization of N-form formation, spores of *K. viridifaciens* were pre-germinated in TSBS (i.e. TSB containing 10% sucrose) for 5 hours. Aliquots of 10 μl of the recovered germlings were placed in an ibiTreat 35 mm low imaging dish (ibidi®), after which an LPMA patch was placed on top of the germlings. For visualization of

N-form growth, 50 µl aliquots of filtered N-forms were used. All samples were imaged for ~15 hours using an inverted Zeiss Axio Observer Z1 microscope equipped with a Temp Module S (PECON) stage-top set to 30°C. Z-stacks with a 1 µm spacing were taken every six minutes using a 40x water immersion objective. Average intensity projections of the in-focus frames were used to compile the final movies. Light intensity over time was equalised using the correct bleach plugin of ImageJ (version 1.51f).

To visualize the proliferation of *alpha* or filtered N-forms, cells were collected and resuspended in 300 µl LPB (containing 4-22% sucrose) and placed in the wells of a chambered 8-well µ-slide (ibidi®). Cells were imaged on a Nikon Eclipse Ti-E inverted microscope equipped with a confocal spinning disk unit (CSU-X1) operated at 10,000 rpm (Yokogawa), using a 40x Plan Fluor Lens (Nikon) and illuminated in bright-field. Images were captured every 2 minutes for 10-15 hours by an Andor iXon Ultra 897 High Speed EM-CCD camera (Andor Technology). Z-stacks were acquired at 0.2-0.5 µm intervals using a NI-DAQ controlled Piezo element. During imaging wall-less cells were kept at 30 °C using INUG2E-TIZ stage top incubator (Tokai Hit).

Electron microscopy

For transmission electron microscopy, L-forms obtained from a 7-day-old liquid culture of the *K. viridifaciens alpha* strain were trapped in agarose blocks prior to fixation with 1.5% glutaraldehyde. In contrast, cultures of the wild-type strain forming N-forms were immediately fixed for an hour with 1.5% glutaraldehyde before being filtered (see above). Filtered N-forms were then washed twice with 1X PBS prior to embedding in 2% low melting agarose. A post-fixation step with 1% OsO_4 was performed on both L- and N-forms. Samples were embedded in Epon and sectioned

into 70 nm slices. Samples were stained using uranyl-acetate (2%) and lead-citrate (0.4%) if necessary. Samples were imaged using a Jeol 1010 or a Fei 12 BioTwin transmission electron microscope.

Genome sequencing and SNP analysis

For genomic DNA isolation, the stable L-form cell line *alpha* was grown in LPB medium for 3 days. After harvesting of the cells by centrifugation, genomic DNA was isolated as described[50]. Whole-genome sequencing and SNP analyses were performed by BaseClear (Leiden, The Netherlands), using the sequence of the parental strain as a reference[33].

DivIVA detection using Western analysis

To detect DivIVA using Western analysis, biomass of L-form strains was harvested after 7 days of growth in LPB medium (100 rpm), while biomass of mycelial strains was obtained from TSBS medium (200 rpm) after 17 hours. Cell pellets were washed twice with 10% PBS, after which they were resuspended in 50mM HEPES pH 7.4, 50 mM NaCl, 0.5% Triton X-100, 1 mM PFMS and P8465 protease inhibitor cocktail (Sigma). The cells and mycelia were disrupted with a Bioruptor Plus Sonication Device (Diagenode). Complete lysis was checked by microscope, after which the soluble cell lysate was separated by centrifugation at 13,000 rpm for 10 min at 4°C. The total protein concentration in the cell lysates was quantified by BCA assay (Sigma-Aldrich). Equal amounts of total proteins were separated with SDS-PAGE using 12,5% gels. Proteins were transferred to polyvinylidene difluoride (PVDF) membranes (GE Healthcare) with the Mini Trans-Blot® Cell (Bio-Rad Laboratories) according to the manufacturer's instructions. DivIVA was detected using a 1:5,000

dilution of polyclonal antibodies raised against *Corynebacterium glutamicum* DivIVA, and kindly provided by Professor Bramkamp (Ludwig-Maximilian-Universität München). The secondary antibody, anti-rabbit IgG conjugated to alkaline phosphatase (Sigma), was visualized with the BCIP/NBT Color Development Substrate (Promega).

REFERENCES

1 Kysela, D. T., Randich, A. M., Caccamo, P. D. & Brun, Y. V. Diversity takes shape: understanding the mechanistic and adaptive basis of bacterial morphology. *PLoS Biol* **14**, e1002565, doi:10.1371/journal.pbio.1002565 (2016).

2 Cabeen, M. T. & Jacobs-Wagner, C. Bacterial cell shape. *Nat Rev Microbiol* **3**, 601-610, doi:10.1038/nrmicro1205 (2005).

3 Typas, A., Banzhaf, M., Gross, C. A. & Vollmer, W. From the regulation of peptidoglycan synthesis to bacterial growth and morphology. *Nat Rev Microbiol* **10**, 123-136, doi:10.1038/nrmicro2677 (2012).

4 Park, J. T. & Strominger, J. L. Mode of action of penicillin. *Science* **125**, 99-101 (1957).

5 Cho, H., Uehara, T. & Bernhardt, T. G. Beta-lactam antibiotics induce a lethal malfunctioning of the bacterial cell wall synthesis machinery. *Cell* **159**, 1300-1311, doi:10.1016/j.cell.2014.11.017 (2014).

6 Meeske, A. J. *et al.* SEDS proteins are a widespread family of bacterial cell wall polymerases. *Nature* **537**, 634-638, doi:10.1038/nature19331 (2016).

7 Szwedziak, P. & Löwe, J. Do the divisome and elongasome share a common evolutionary past? *Curr Opin Microbiol* **16**, 745-751, doi:10.1016/j.mib.2013.09.003 (2013).

8 Höltje, J. V. Growth of the stress-bearing and shape-maintaining murein sacculus of *Escherichia coli*. *Microbiol Mol Biol Rev* **62**, 181-203 (1998).

9 Claessen, D., Rozen, D. E., Kuipers, O. P., Sogaard-Andersen, L. & van Wezel, G. P. Bacterial solutions to multicellularity: a tale of biofilms, filaments and fruiting bodies. *Nat Rev Microbiol* **12**, 115-124, doi:10.1038/nrmicro3178 (2014).

10 Flärdh, K. & Buttner, M. J. *Streptomyces* morphogenetics: dissecting differentiation in a filamentous bacterium. *Nat Rev Microbiol* **7**, 36-49 (2009).

11 Vicente, M. & Errington, J. Structure, function and controls in microbial division. *Mol Microbiol* **20**, 1-7 (1996).

12 Tamames, J., González-Moreno, M., Mingorance, J., Valencia, A. & Vicente, M. Bringing gene order into bacterial shape. *Trends Genet* **17**, 124-126 (2001).

13 Marston, A. L., Thomaides, H. B., Edwards, D. H., Sharpe, M. E. & Errington, J. Polar localization of the MinD protein of *Bacillus subtilis* and its role in selection of the mid-cell division site. *Genes Dev* **12**, 3419-3430 (1998).

14 Flärdh, K. Essential role of DivIVA in polar growth and morphogenesis in *Streptomyces coelicolor* A3(2). *Mol Microbiol* **49**, 1523-1536 (2003).

15 Holmes, N. A. *et al.* Coiled-coil protein Scy is a key component of a multiprotein assembly controlling polarized growth in *Streptomyces*. *Proc Natl Acad Sci U S A* **110**, E397-406, doi:10.1073/pnas.1210657110 (2013).

16 Letek, M. *et al.* DivIVA is required for polar growth in the MreB-lacking rod-shaped actinomycete *Corynebacterium glutamicum*. *J Bacteriol* **190**, 3283-3292, doi:10.1128/JB.01934-07 (2008).

17 McCormick, J. R. Cell division is dispensable but not irrelevant in *Streptomyces*. *Curr Opin Biotechnol* **12**, 689-698, doi:10.1016/j.mib.2009.10.004 (2009).

18 McCormick, J. R., Su, E. P., Driks, A. & Losick, R. Growth and viability of *Streptomyces coelicolor* mutant for the cell division gene *ftsZ*. *Mol Microbiol* **14**, 243-254 (1994).

19 Klieneberger, E. The natural occurrence of pleuropneumonia-like organisms in apparent symbiosis with *Streptobacillus moniliformis* and other bacteria. *J Pathol Bacteriol* **40**, 93-105 (1935).

20 Leaver, M., Dominguez-Cuevas, P., Coxhead, J. M., Daniel, R. A. & Errington, J. Life without a wall or division machine in *Bacillus subtilis*. *Nature* **457**, 849-853, doi:10.1038/nature07742 (2009).

21 Frenkel, A. & Hirsch, W. Spontaneous development of L forms of Streptococci requiring secretions of other bacteria or sulphydryl compounds for normal growth. *Nature* **191**, 728-730 (1961).

22 Studer, P. *et al.* Proliferation of *Listeria monocytogenes* L-form cells by formation of internal and external vesicles. *Nat Commun* **7**, 13631, doi:10.1038/ncomms13631 (2016).

23 Dienes, L. The Isolation of L type cultures from *Bacteroides* with the aid of penicillin and their reversion into the usual bacilli. *J Bacteriol* **56**, 445-456 (1948).

24 Burmeister, H. R. & Hesseltine, C. W. Induction and propagation of a *Bacillus subtilis* L form in natural and synthetic media. *J Bacteriol* **95**, 1857-1861 (1968).

25 Dell'Era, S. *et al. Listeria monocytogenes* L-forms respond to cell wall deficiency by modifying gene expression and the mode of division. *Mol Microbiol* **73**, 306-322, doi:10.1111/j.1365-2958.2009.06774.x (2009).

26 Domínguez-Cuevas, P., Mercier, R., Leaver, M., Kawai, Y. & Errington, J. The rod to L-form transition of *Bacillus subtilis* is limited by a requirement for the protoplast to escape from the cell wall sacculus. *Mol Microbiol* **83**, 52-66, doi:10.1111/j.1365-2958.2011.07920.x (2012).

27 Errington, J., Mickiewicz, K., Kawai, Y. & Wu, L. J. L-form bacteria, chronic diseases and the origins of life. *Philosophical Transactions of the Royal Society B: Biological Sciences* **371**, doi:10.1098/rstb.2015.0494 (2016).

28 Mercier, R., Kawai, Y. & Errington, J. Excess membrane synthesis drives a primitive mode of cell proliferation. *Cell* **152**, 997-1007, doi:10.1016/j.cell.2013.01.043 (2013).

29 Kawai, Y. *et al.* Cell growth of wall-free L-form bacteria is limited by oxidative damage. *Curr Biol* **25**, 1613-1618, doi:10.1016/j.cub.2015.04.031 (2015).

30 Mercier, R., Kawai, Y. & Errington, J. General principles for the formation and proliferation of a wall-free (L-form) state in bacteria. *Elife* **3**, doi:10.7554/eLife.04629 (2014).

31 Errington, J. L-form bacteria, cell walls and the origins of life. *Open Biol* **3**, 120143, doi:10.1098/rsob.120143 (2013).

32 Girard, G. *et al.* Analysis of novel kitasatosporae reveals significant evolutionary changes in conserved developmental genes between *Kitasatospora* and *Streptomyces*. *Antonie Van Leeuwenhoek* **106**, 365-380, doi:10.1007/s10482-014-0209-1 (2014).

33 Ramijan, A. K., van Wezel, G. P. & Claessen, D. Genome sequence of the filamentous actinomycete *Kitasatospora viridifaciens*. *Genome Announc*, In press (2016).

34 Peschel, A. *et al. Staphylococcus aureus* resistance to human defensins and evasion of neutrophil killing via the novel virulence factor MprF is based on modification of membrane lipids with l-lysine. *J Exp Med* **193**, 1067-1076 (2001).

35 Maloney, E. *et al.* The two-domain LysX protein of *Mycobacterium tuberculosis* is required for production of lysinylated phosphatidylglycerol and resistance to cationic antimicrobial peptides. *PLoS Pathog* **5**, e1000534, doi:10.1371/journal.ppat.1000534 (2009).

36 El Ghachi, M., Bouhss, A., Blanot, D. & Mengin-Lecreulx, D. The *bacA* gene of *Escherichia coli* encodes an undecaprenyl pyrophosphate phosphatase activity. *J Biol Chem* **279**, 30106-30113, doi:10.1074/jbc.M401701200 (2004).

37 Celler, K., Koning, R. I., Willemse, J., Koster, A. J. & van Wezel, G. P. Cross-membranes orchestrate compartmentalization and morphogenesis in *Streptomyces*. *Nat Commun* **7**, ncomms11836, doi:10.1038/ncomms11836 (2016).

38 Barka, E. A. *et al.* Taxonomy, physiology, and natural products of *Actinobacteria*. *Microbiol Mol Biol Rev* **80**, 1-43, doi:10.1128/MMBR.00019-15 (2016).

39 Seipke, R. F., Kaltenpoth, M. & Hutchings, M. I. *Streptomyces* as symbionts: an emerging and widespread theme? *FEMS Microbiol Rev* **36**, 862-876, doi:10.1111/j.1574-6976.2011.00313.x (2012).

40 Amijee, F., Allans, E. J., Waterhouse, R. N., Glover, L. A. & Paton, A. M. Non-pathogenic association of L-form bacteria (*Pseudomonas syringae* pv. *phaseolicola*) with bean plants (*Phaseolus vulgaris* L.) and its potential for biocontrol of halo blight disease. *Biocontrol Sci Technol* **2**, 203-214 (1992).

41 Allan, E. J., Hoischen, C. & Gumpert, J. Bacterial L-forms. *Adv Appl Microbiol* **68**, 1-39, doi:10.1016/S0065-2164(09)01201-5 (2009).

42 Viaene, T., Langendries, S., Beirinckx, S., Maes, M. & Goormachtig, S. *Streptomyces* as a plant's best friend? *FEMS Microbiol Ecol* **92**, doi:10.1093/femsec/fiw119 (2016).

43 Stuttard, C. Temperate phages of *Streptomyces venezuelae*: lysogeny and host specificity shown by phages SV1 and SV2. *Journal of General Microbiology* **128**, 115-121 (1982).

44 Innes, C. M. J. & Allan, E. J. Induction, growth and antibiotic production of *Streptomyces viridifaciens* L-form bacteria. *J Appl Microbiol* **90**, 301-308 (2001).

45 Sun, J., Kelemen, G. H., Fernández-Abalos, J. M. & Bibb, M. J. Green fluorescent protein as a reporter for spatial and temporal gene expression in *Streptomyces coelicolor* A3(2). *Microbiology* **145**, 2221-2227 (1999).

46 Gust, B., Challis, G. L., Fowler, K., Kieser, T. & Chater, K. F. PCR-targeted *Streptomyces* gene replacement identifies a protein domain needed for biosynthesis of the sesquiterpene soil odor geosmin. *Proc Natl Acad Sci U S A* **100**, 1541-1546, doi:10.1073/pnas.0337542100 (2003).

47 Vara, J., Lewandowska-Skarbek, M., Wang, Y. G., Donadio, S. & Hutchinson, C. R. Cloning of genes governing the deoxysugar portion of the erythromycin biosynthesis pathway in S*accharopolyspora erythraea* (*Streptomyces erythreus*). *J Bacteriol* **171**, 5872-5881 (1989).

48 Świątek, M. A., Tenconi, E., Rigali, S. & van Wezel, G. P. Functional analysis of the N-acetylglucosamine metabolic genes of *Streptomyces coelicolor* and role in control of development and antibiotic production. *J Bacteriol* **194**, 1136-1144, doi:10.1128/JB.06370-11 (2012).

49 Redenbach, M. *et al.* A set of ordered cosmids and a detailed genetic and physical map for the 8 Mb *Streptomyces coelicolor* A3(2) chromosome. *Mol Microbiol* **21**, 77-96 (1996).

50 Kieser, T., Bibb, M. J., Buttner, M. J., Chater, K. F. & Hopwood, D. A. *Practical Streptomyces genetics*. (The John Innes Foundation, 2000).

Acknowledgements

We would like to thank Tim Janson for microscopy support and Marc Bramkamp for providing us with antibodies. We are indebted to Mark Leaver, Roberto Kolter, Danny Rozen, Ben Lugtenberg and Paul Hooykaas for critical reading of the manuscript. This work was supported by a VIDI grant from the Dutch Applied Research Council (STW 12957).

Author Contributions

K.R., J.W., E.U., A.J.W., A.M., A.B., D.H., G.P.W. and D.C. collected the data and aided in data analysis. D.C. and G.P.W. designed the experiments and supervised the research. K.R., G.P.W. and D.C. wrote the manuscript with input from all co-authors.

Competing Financial Interests

The authors declare there are no competing financial interests

LEGENDS

Figure 1. Wall-less cells are a natural stage in bacterial development.

(A) In media containing high levels of sucrose, the filamentous bacterium *K. viridifaciens* forms spherical vesicles (arrowheads), which stain with the dye SYTO9 (B). Transmission electron micrographs indicate that these vesicles are cells that lack the cell wall (C, D). The arrowheads indicate the cell membrane. (E) These wall-less cells (arrows) are extruded from the hyphal tip. Arrowheads indicate new branches, while “S” designates the spore. Images were taken from Extended Data Video S1. (F) Phase-contrast images from Extended Data Video S3 showing proliferation of wall-less cells in LPB medium. The times are indicated in HH:MM. The cell indicated with

an asterisk had entered the field after 38 mins. (G) Reversion of wall-less cells to hyphal growth yields colonies consisting of hyphae and (newly-formed) wall-less cells. Images were taken from Extended Data Video S4. (H) Model indicating that wall-less cells (or N-forms) are a natural stage in bacterial development. On osmo-protective media, vegetative hyphae generate N-form cells that either proliferate transiently in the wall-less state, or immediately revert to mycelial growth (right). Reversion to mycelial growth allows the strain to complete its canonical life cycle (left). Scale bars represent 1 µm (D), 5 µm (C, F), 10 µm (A, B, E) or 20 µm (G).

Figure 2. Characterization of the stable L-form cell line *alpha*. (A) Phase-contrast images from Extended Data Video S6, which demonstrate the proliferation of *alpha* in the L-form state. The arrowhead points to the dividing mother cell. Please note that after the generation of new progeny the mother cell lysis (indicated with an asterisk). (B) Transmission electron micrograph showing an *alpha* cell lacking the cell wall. (C) On plates containing sucrose and $MgCl_2$, *alpha* forms colonies exclusively containing L-forms, while it forms mycelial colonies on plates without these supplements. (D) L-forms of *alpha* (*alpha*^{L}) transformed with pGreen, leading to the constitutive expression of eGFP, show a diffuse cytosolic GFP signal. By contrast, L-form cells containing pKR3, thereby expressing eGFP fused to DivIVA, show distinct foci localized to the membrane. When the strains are grown as a mycelium (*alpha*^{M}), DivIVA-eGFP localized to the hyphal tips (arrowheads). No fluorescence is observed in cells or mycelium containing the control plasmid pKR1. Scale bars represent 500 nm (B), 5 µm (A), 10 µm (D) or 20 µm (C).

Figure 3. Reversible metamorphosis depends on DivIVA. (A) Illustration of the *dcw* clusters in *alpha* and the derivative strains lacking *divIVA* or part of the *dcw* cluster. (B) Western analysis confirming the absence of DivIVA in the Δ*divIVA* and Δ*dcw* mutants. Introduction of *divIVA* under control of its own (pKR6) or the *gap1* (pKR7) promoter restores the presence of DivIVA. Likewise, introduction of the *S. coelicolor dcw* gene cluster (on pKR8) in the Δ*divIVA* or Δ*dcw* mutant strains restores the presence of DivIVA. MW is the molecular weight in kDa. (C) Comparable growth between *alpha* (solid black line) and the Δ*divIVA* (dashed line) and the Δ*dcw* mutants (dotted line) in liquid LPB medium. (D) The mutant strains lacking *divIVA* can no longer grow on MYM plates lacking sucrose and $MgCl_2$. (D) Reintroduction of the *S. coelicolor dcw* gene cluster (on pKR8) in the Δ*dcw* mutant restores mycelial growth, including septal PG synthesis, as revealed by staining with fluorescent vancomycin (vanFL). Scale bar represents 5 μm.

Extended Data Figure S1. Osmolytes are required for the formation of wall-less cells. The addition of 0.6M sucrose (A) or NaCl (B) to LPB medium is required for the formation of wall-less cells. No wall-less cells are detected without the addition of osmolytes (C). Scale bars represent 20 μm.

Extended Data Figure S2. Formation of wall-less cells in *Streptomyces* and *Kitasatospora* species. Unlike *Streptomyces coelicolor* (A), *Streptomyces lividans* (B) and *Streptomyces griseus* (C), wall-less (arrowheads) are evident in *Streptomyces venezuelae* (D), and *Kitasatospora* strains MBT63 (E) and MBT66 (F) grown in LPB medium. The inlays show magnified versions of wall-less cells in these species. (G-I).

688 Visualization of DNA in wall-less cells using SYTO9. Scale bars represent 5 µm
689 (inlays), 10 µm (G-I) or 20 µm (A-F).
690
691 **Extended Data Figure S3. Reversible metamorphosis in the *K. viridifaciens* Δ*ssgB***
692 **mutant.** (A) Deletion of *ssgB* in *K. viridifaciens* blocks the formation of grey spores.
693 (B, C) Transmission electron micrographs of N-forms of the Δ*ssgB* mutant strain
694 indicates that they lack the cell wall. The arrowhead indicates the cell membrane (C).
695 (D) Phase-contrast images from Extended Data Video S5 showing N-form
696 proliferation in liquid medium. The times are indicated in HH:MM. (E) Plating of N-
697 forms of the *ssgB* mutant on LPMA yields colonies consisting of mycelia and N-
698 forms. Scale bars represent 200 nm (C), 2 µm (B), 10 µm (D) or 20 µm (E).
699
700 **Extended Data Figure S4. Functional complementation of the Δ*divIVA* mutant**
701 **by DivIVA-eGFP** The DivIVA-eGFP fusion expressed from pKR3 restores
702 filamentous growth of the *divIVA* mutant, and localizes to the hyphal tips
703 (arrowheads). Scale bars represent 10 µm.
704
705 **Extended Data Video S1. Apical extrusion of N-forms in *K. viridifaciens*.** N-forms
706 are extruded from the hyphal tip after 430 min, coinciding with a transient arrest in tip
707 growth. After extrusion of the N-forms, the hypha resumes elongation after 540 min,
708 while subapically new branches become visible after 620 min. The times are indicated
709 in min.
710 **Extended Data Video S2. Extrusion of N-forms from branches in *K. viridifaciens.***
711 N-forms are extruded from the tips of branches that are formed subapically.
712

713 **Extended Data Video S3. Proliferation of N-forms.** N-forms from *K. viridifaciens*
714 proliferate in the wall-less state in liquid LPB medium. The arrowhead indicates the
715 cells that are shown in Fig. 1F. The times are indicated in HH:MM. The scale bar
716 represents 10 µm.
717
718 **Extended Data Video S4. Proliferation and reversion of wild-type N-forms.**
719 Growth and reversion of N-forms on solid LPMA medium yields colonies consisting
720 of both hyphae and N-forms. The times are indicated in HH:MM. The scale bar
721 indicates 20 µm.
722
723 **Extended Data Video S5. Proliferation of N-forms of the Δ*ssgB* mutant strain.** N-
724 forms of the Δ*ssgB* mutant strain proliferate in the wall-less state in liquid LPB
725 medium. The arrowhead indicates the cell that is shown in Extended Data Fig. S3D.
726 The times are indicated in HH:MM. The scale bar represents 10 µm.
727
728 **Extended Data Video S6. Proliferation of *alpha* in the L-form state.** The stable
729 cell line *alpha* exclusively proliferates in the L-form state in medium containing high
730 levels of sucrose. The arrowhead indicates the proliferating cell that is used to make
731 Fig. 2A. The times are indicated in HH:MM. The scale bar represents 10 µm.
732
733 **Extended Data Video S7. L-forms are released from hyphal tips in *alpha*.**
734 Transfer of mycelial colonies of *alpha* on plates containing high levels of sucrose
735 leads to the extrusion of L-forms from the hyphal tips. The times are indicated in min.

Extended Data Table 1. Detected single nucleotide polymorphisms (SNPs) in the chromosome of *alpha*.

SNP	Position in genome	Locus	Variant in wild-type	Variant in *alpha*	Effect on protein	Protein function
1	546 832	NCR	C	A	None	Unknown
2	3 549 271	BOQ63_22710	G	A	$LysX^{T183I}$	Biosynthesis of lysyl-phosphatidyl glycerol
3	3 297 354	BOQ63_21575	C	A	$UppP^{L58M}$	Dephosphorylation of undecaprenyl pyrophosphate

NCR: non-coding region. LysX: phosphatidylglycerol lysyltransferase, UppP: undecaprenyl diphosphatase.

Extended Data Table 2. Strains used in this study.

Strains	Genotype	Reference
Escherichia coli strains		
DH5α	F$^-$ Φ80'*lacZ*ΔM15 Δ(*lacZYA-argF*)U169 *recA1 endA1 hsdR17*(rK$^-$, mK$^+$) *phoA supE44 thi-1 gyrA96 relA1* λ$^-$	[1]
JM109	*recA1 endA1 gyrA96 thi hsdR17 supE44 relA1* λ$^-$ Δ(*lac-proAB*) [F' *traD36 proAB lacI*^{q}ZΔM15]	[2]
ET12567	F$^-$ *dam-13::*Tn9 (Chl^R) *dcm-6 hsdM hsdR recF143 zjj- 201::*Tn10 *galK2 galT22 ara14 lacY1 xyl-5 leuB6 thi-1 tonA31 rpsL136 hisG4 tsx78 mtl-1 glnV44*	[3]
SCS110	*rpsL* (Str^R) *thr leu endA thi-1 lacY galK galT ara tonA tsx dam dcm supE*44 Δ(*lac-proAB*) [*F' traD*36 *proAB lacI*^{q}ZΔM15]	[4]
Streptomyces/Kitasatospora strains		
Streptomyces coelicolor A3(2) M145	Wild-type	Lab collection
Streptomyces lividans 1326	Wild-type	Lab collection
Streptomyces griseus	Wild-type	Lab collection
Streptomyces venezuelae DIVERSA	Wild-type	Lab collection
Kitasatospora viridifaciens DSM40239	Wild-type	Lab collection
Kitasatospora sp. MBT63	Wild-type	[5]
Kitasatospora sp. MBT66	Wild-type	[5]
K. viridifaciens Δ*ssgB*	*K. viridifaciens* DSM40239 derivative in which the *ssgB* gene has been replaced by an apramycin resistance marker	This work
K.viridifacienes L-form strains		
alpha	Stable *K.viridifaciens* L-form cell line	This work
Δ*divIVA*	*alpha* derivative in which the *divIVA* gene has been replaced by an apramycin resistance marker	This work
Δ*dcw*	*alpha* derivative in which part of the *dcw* gene cluster has been replaced by an apramycin resistance marker. The deleted genes include *ftsW, murG, ftsQ, ftsZ, ylmD, ylmE, sepG, sepF,* and *divIVA*.	This work

References

1 Hanahan, D. Studies on transformation of *Escherichia coli* with plasmids. *J Mol Biol* **166**, 557-580 (1983).

2 Yanisch-Perron, C., Vieira, J. & Messing, J. Improved M13 phage cloning vectors and host strains: nucleotide sequences of the M13mp18 and pUC19 vectors. *Gene* **33**, 103-119 (1985).

3 MacNeil, D. J. *et al.* Analysis of *Streptomyces avermitilis* genes required for avermectin biosynthesis utilizing a novel integration vector. *Gene* **111**, 61-68 (1992).

4 Jerpseth, B. & Kretz, B. L. SCS110: *dam-, dcm-, endA-* Epicurian coli® competent cells. *Strategies* **6**, 22 (1993).

5 Girard, G. *et al.* Analysis of novel kitasatosporae reveals significant evolutionary changes in conserved developmental genes between *Kitasatospora* and *Streptomyces*. *Antonie Van Leeuwenhoek* **106**, 365-380, doi:10.1007/s10482-014-0209-1 (2014).

Extended Data Table 3. Plasmids used in this study.

Plasmid	Description and relevant features	Reference
pWHM3	Unstable, multi-copy and self-replicating S*treptomyces* vector. Contains thiostrepton and ampicillin resistance cassette.	[1]
pIJ780	Plasmid containing a viomycin (*vph*) resistance cassette.	[2]
pIJ8600	*E. coli–Streptomyces* shuttle vector containing the φC31 *attP-int* region for genomic integration. Confers resistance to apramycin and thiostrepton.	[3]
pIJ8630	*E. coli–Streptomyces* shuttle vector containing the φC31 *attP-int* region for genomic integration. Confers resistance to apramycin	[3]
pGreen	pIJ8630 containing the *eGFP* gene under control of the constitutive *gap1* promoter of *S. coelicolor.*	[4]
ST4A10	Supercosmid fragment containing SCO2068-SCO2105 (43 147bp). Confers resistance to ampicillin and kanamycin.	[5]
pKR1	pWHM3 containing the flanking regions of the *K. viridifaciens ssgB* gene interspersed by the *apra-loxP* cassette.	This study
pKR2	pIJ8630 derivative containing the viomycin resistance cassette from pIJ780 cloned into the unique NheI site.	This work
pKR3	pKR2 derivative containing a C-terminal *eGFP* fusion to *divIVA* of *K. viridifaciens* under control of the *gap1* promoter of *S. coelicolor.*	This work
pKR4	pWHM3 containing the flanking regions of the *K. viridifaciens divIVA* gene interspersed by the *apra-loxP* cassette.	This work
pKR5	pWHM3 derivative containing the flanking regions around the *K. viridifaciens dcw* gene cluster interspersed by the *apra-loxP* cassette.	This work
pKR6	pIJ8600 containing *divIVA* of *K. viridifaciens* under control of its native promoter (which includes the coding sequences of *sepF* and *sepG*).	This work
pKR7	pIJ8600 containing the *divIVA* gene of *K. viridifaciens* under control of the *gap1* promoter of *S. coelicolor*.	This work
pKR8	pIJ8600 containing a 13,268 bp BglII fragment encompassing the *murD*, *ftsW*, *murG*, *ftsQ*, *ftsZ*, *ylmD*, *ylmE*, *sepF*, *sepG* and *divIVA* genes of the *S. coelicolor dcw* gene cluster.	This work

References

1 Vara, J., Lewandowska-Skarbek, M., Wang, Y. G., Donadio, S. & Hutchinson, C. R. Cloning of genes governing the deoxysugar portion of the erythromycin biosynthesis pathway in S*accharopolyspora erythraea* (*Streptomyces erythreus*). *J Bacteriol* **171**, 5872-5881 (1989).

2 Gust, B., Challis, G. L., Fowler, K., Kieser, T. & Chater, K. F. PCR-targeted *Streptomyces* gene replacement identifies a protein domain needed for biosynthesis of the sesquiterpene soil odor geosmin. *Proc Natl Acad Sci U S A* **100**, 1541-1546, doi:10.1073/pnas.0337542100 (2003).

3 Sun, J., Kelemen, G. H., Fernández-Abalos, J. M. & Bibb, M. J. Green fluorescent protein as a reporter for spatial and temporal gene expression in *Streptomyces coelicolor* A3(2). *Microbiology* **145**, 2221-2227 (1999).

4 Zacchetti, B. *et al.* Aggregation of germlings is a major contributing factor towards mycelial heterogeneity of *Streptomyces*. *Sci Rep* **6**, 27045, doi:10.1038/srep27045 (2016).

5 Redenbach, M. *et al.* A set of ordered cosmids and a detailed genetic and physical map for the 8 Mb *Streptomyces coelicolor* A3(2) chromosome. *Mol Microbiol* **21**, 77-96 (1996).

Extended Data Table 4. Primers used in this study.
Restriction sites are underlined.

Primer	Sequence (5' – 3')
P1-*ssgB*-FW	GACGAATTCAGGCGTCAGAAACGGGTATC
P2-*ssgB*-RV	GAAGTTATCCATCACCTCTAGAGCTGACCGTGGTGTTCATAAGC
P3-*ssgB*-FW	GAAGTTATCGCGCATCTCTAGACTGAGCTCTCCGGAAGGAGAA
P4-*ssgB*-RV	GACAAGCTTTCTACCTGACCGGGCTGTT
Delcheck-*ssgB*-FW	GGCGGGTACTCCGTGATGATTC
Delcheck-*ssgB*-RV	AGCTTTCGGCGAGGATGTGG
vph-FW-NheI	GACGCTAGCGGCTGACGCCGTTGGATACACCAAG
vph-RV-NheI	GACGCTAGCAATCGACTGGCGAGCGGCATCCTAC
P_{Gap1}-FW-BglII	GATTACAGATCTCCGAGGGCTTCGAGACC
P_{Gap1}-RV-XbaI	GATGACTCTAGACCGATCTCCTCGTTGGTAC
divIVA-FW-XbaI	GTCAAGCTTCTAGAATGCCATTGACCCCCGAGGA
divIVA-Nostop-RV-NdeI	GACCATATGGTTGTCGCCGTCCTCGTCAATCAGG
P1-*divIVA*-FW	GACGACGAATTCTGTGATGACCGTCGCTCCACTG
P2-*divIVA*-RV	GACGACTCTAGACTTCCGCATGTTGGCCTGGTTC
P1-*dcw*-FW	GACGAATTCTCCGCGAGGTCACGTACATC
P2-*dcw*-RV	GACTCTAGAAGAGCACCAGTGCGAGCTTG
P3-*dcw*-FW	GACTCTAGAAGCAGCAGATGGGCAACCAG
P4-*dcw*-RV	GATAAGCTTCCCGGCTACAACCTCAGTTGTC
Delcheck-*divIVA*-FW	TGACCCGGCCACGACTTTAC
Delcheck-*divIVA*-RV	GGACGCCCTCAACAAAC
Delcheck-*dcw*-FW	CCAGAACTGGCTGGATTTCG
Delcheck-*dcw*-RV	GTCTCCAGGTACGACTTCAG
ftsZ-int-FW	ATGTGGGCCGTGAACTCACC
ftsZ-int-Rv	GACCGCACCGAAGATGATG
ftsQ-int-FW	CCTGGGTGGTGTTCTTCTC
ftsQ-int-Rv	CCTGGGTGGTGTTCTTCTC
sepF-sepG-divIVA-FW-BglII	GACGACAGATCTTGTGATGACCGTCGCTCCACTG
sepF-sepG-divIVA-RV-XbaI	GACGACTCTAGAAACAAACCCGGCTACAACCTCAGTTGTC
divIVA-XbaI-FW	GTCAAGCTTCTAGAATGCCATTGACCCCCGAGGA
divIVA-NdeI-RV	GATCGAATTCATATGCCCGGCTACAACCTCAGTTGTC
divIVA seq1-FW	AGCAGCAGATGGGCAACCAG
divIVA seq2-FW	CGCGTCTGAAGTCGTACCTG
divIVA seq-RV	ACCTCGTCCTCGTCATAGC
SCO2079_F-520	TCACGGCGCTGTCGAAGGAGGCCG
SCO2079_R+1162	CTCATCGAGGAAGGCATCGACCTC
$divIVA_{SCO}$-FW	AAGGCTACGCCGTACTACAG
$divIVA_{SCO}$-RV	AGATACGGGCTTGCCGAATG

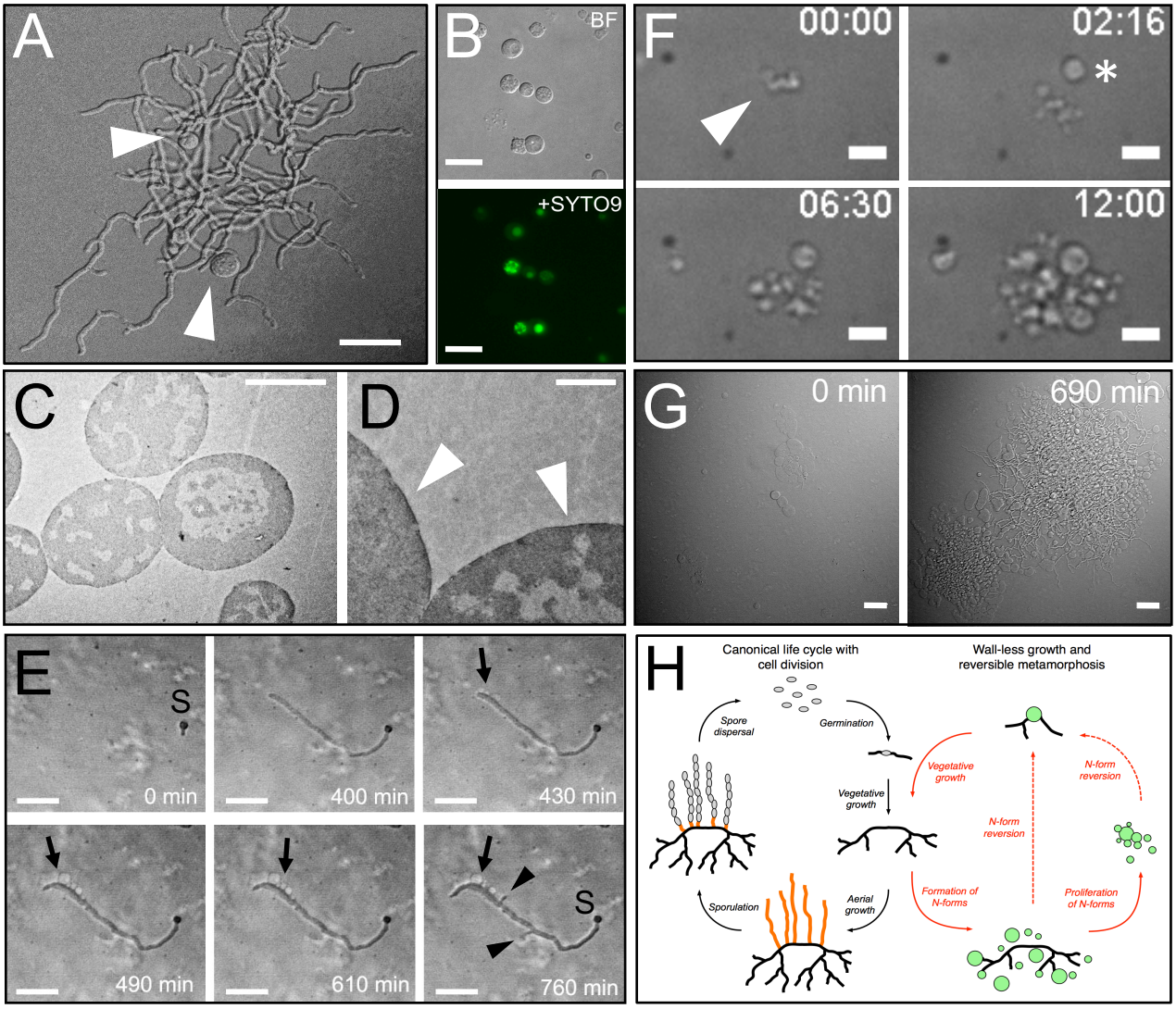

Figure 1. Wall-less cells are a natural stage in bacterial development.
(A) In media containing high levels of sucrose, the filamentous bacterium *K. viridifaciens* forms spherical vesicles (arrowheads), which stain with the dye SYTO9 (B). Transmission electron micrographs indicate that these vesicles are cells that lack the cell wall (C, D). The arrowheads indicate the cell membrane. (E) These wall-less cells (arrows) are extruded from the hyphal tip. Arrowheads indicate new branches, while "S" designates the spore. Images were taken from Extended Data Video S1. (F) Phase-contrast images from Extended Data Video S3 showing proliferation of wall-less cells in LPB medium. The times are indicated in HH:MM. The cell indicated with an asterisk had entered the field after 38 mins. (G) Reversion of wall-less cells to hyphal growth yields colonies consisting of hyphae and (newly-formed) wall-less cells. Images were taken from Extended Data Video S4. (H) Model indicating that wall-less cells (or N-forms) are a natural stage in bacterial development. On osmo-protective media, vegetative hyphae generate N-form cells that either proliferate transiently in the wall-less state, or immediately revert to mycelial growth (right). Reversion to mycelial growth allows the strain to complete its canonical life cycle (left). Scale bars represent 1 µm (D), 5 µm (C, F), 10 µm (A, B, E) or 20 µm (G).

Figure 1

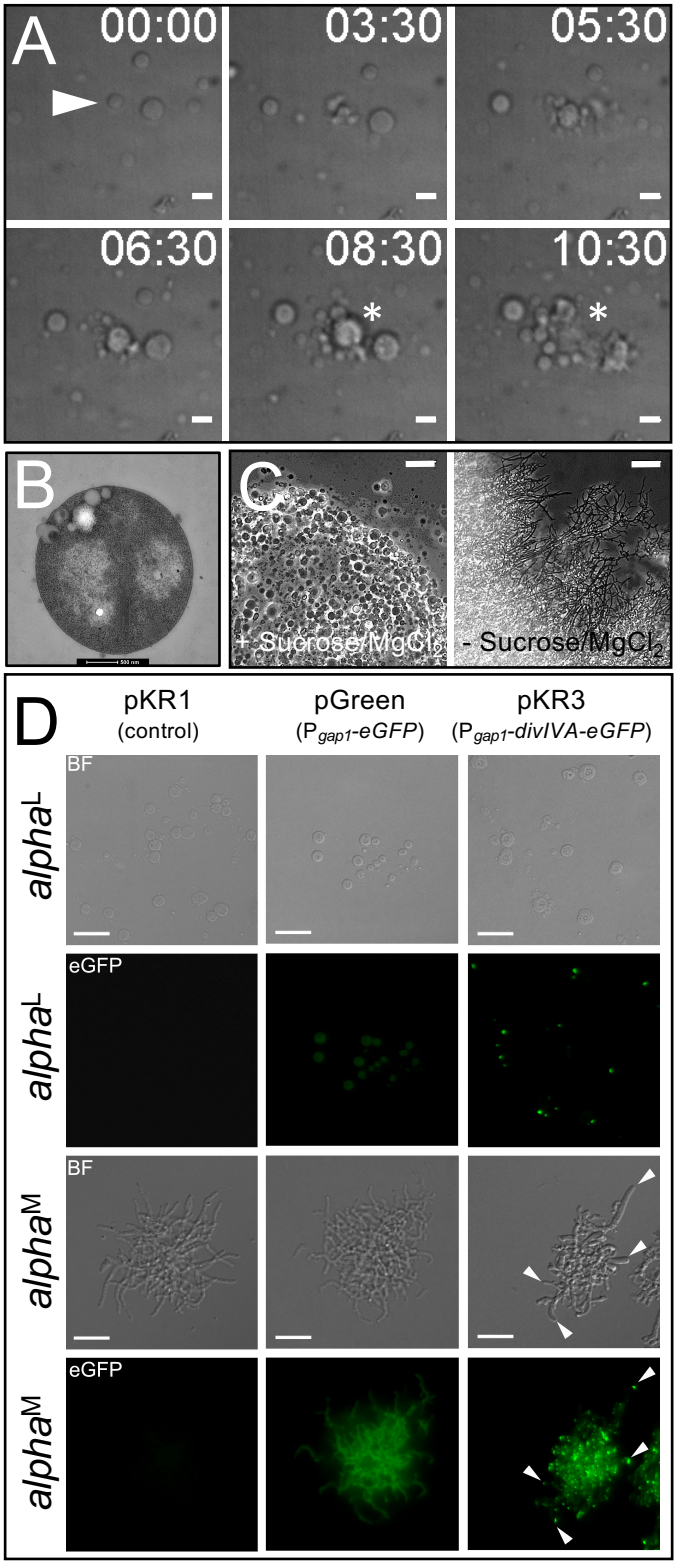

Figure 2. Characterization of the stable L-form cell line *alpha*. (A) Phase-contrast images from Extended Data Video S6, which demonstrate the proliferation of *alpha* in the L-form state. The arrowhead points to the dividing mother cell. Please note that after the generation of new progeny the mother cell lysis (indicated with an asterisk). (B) Transmission electron micrograph showing an *alpha* cell lacking the cell wall. (C) On plates containing sucrose and $MgCl_2$, *alpha* forms colonies exclusively containing L-forms, while it forms mycelial colonies on plates without these supplements. (D) L-forms of *alpha* (*alpha*^{L}) transformed with pGreen, leading to the constitutive expression of eGFP, show a diffuse cytosolic GFP signal. By contrast, L-form cells containing pKR3, thereby expressing eGFP fused to DivIVA, show distinct foci localized to the membrane. When the strains are grown as a mycelium (*alpha*^{M}), DivIVA-eGFP localized to the hyphal tips (arrowheads). No fluorescence is observed in cells or mycelium containing the control plasmid pKR1. Scale bars represent 500 nm (B), 5 µm (A), 10 µm (D) or 20 µm (C).

Figure 2

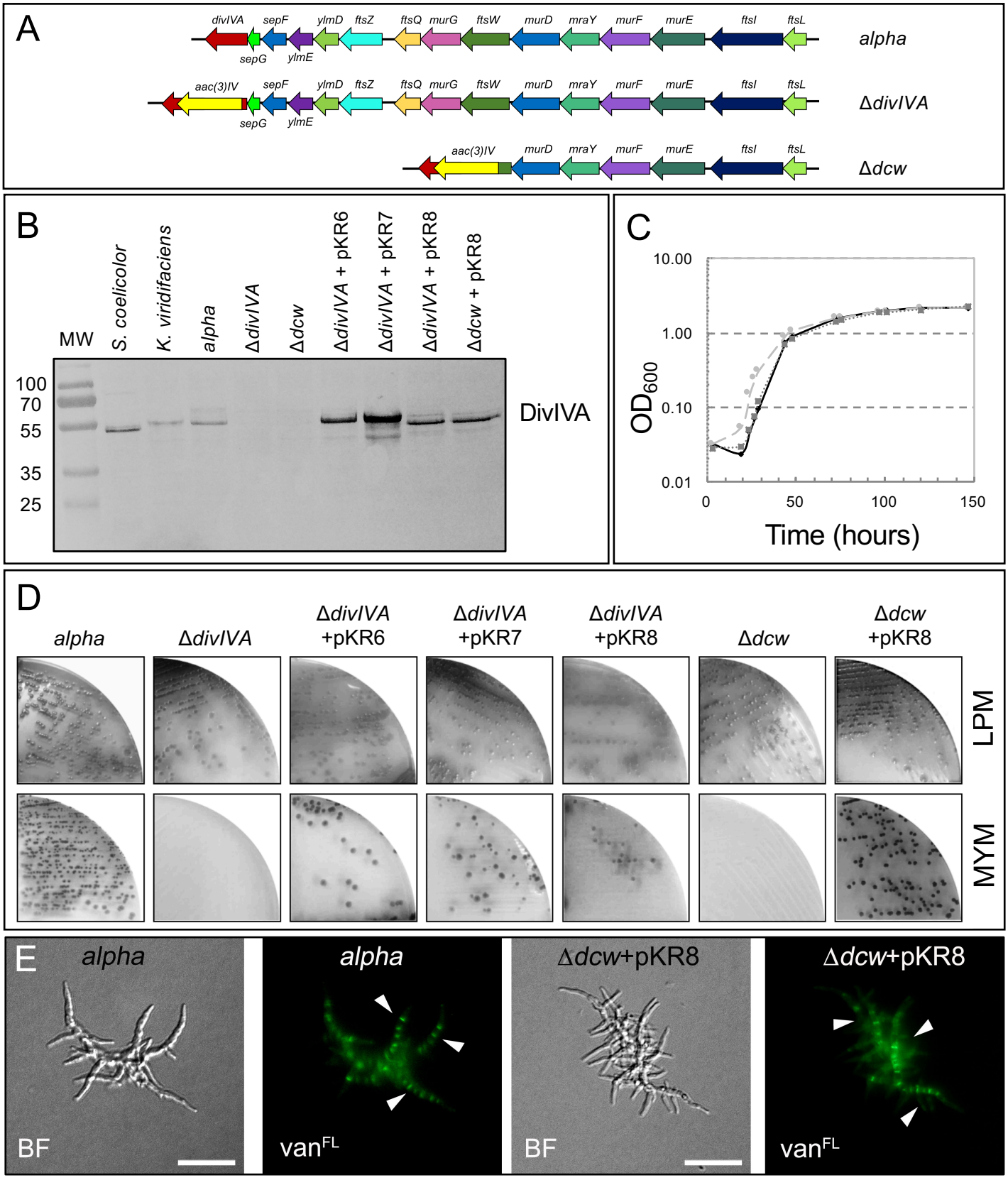

Figure 3. Reversible metamorphosis depends on DivIVA. (A) Illustration of the *dcw* clusters in *alpha* and the derivative strains lacking *divIVA* or part of the *dcw* cluster. (B) Western analysis confirming the absence of DivIVA in the Δ*divIVA* and Δ*dcw* mutants. Introduction of *divIVA* under control of its own (pKR6) or the *gap1* (pKR7) promoter restores the presence of DivIVA. Likewise, introduction of the *S. coelicolor dcw* gene cluster (on pKR8) in the Δ*divIVA* or Δ*dcw* mutant strains restores the presence of DivIVA. MW is the molecular weight in kDa. (C) Comparable growth between *alpha* (solid black line) and the Δ*divIVA* (dashed line) and the Δ*dcw* mutants (dotted line) in liquid LPB medium. (D) The mutant strains lacking *divIVA* can no longer grow on MYM plates lacking sucrose and $MgCl_2$. (D) Reintroduction of the *S. coelicolor dcw* gene cluster (on pKR8) in the Δ*dcw* mutant restores mycelial growth, including septal PG synthesis, as revealed by staining with fluorescent vancomycin (vanFL). Scale bar represents 5 µm.

Figure 3

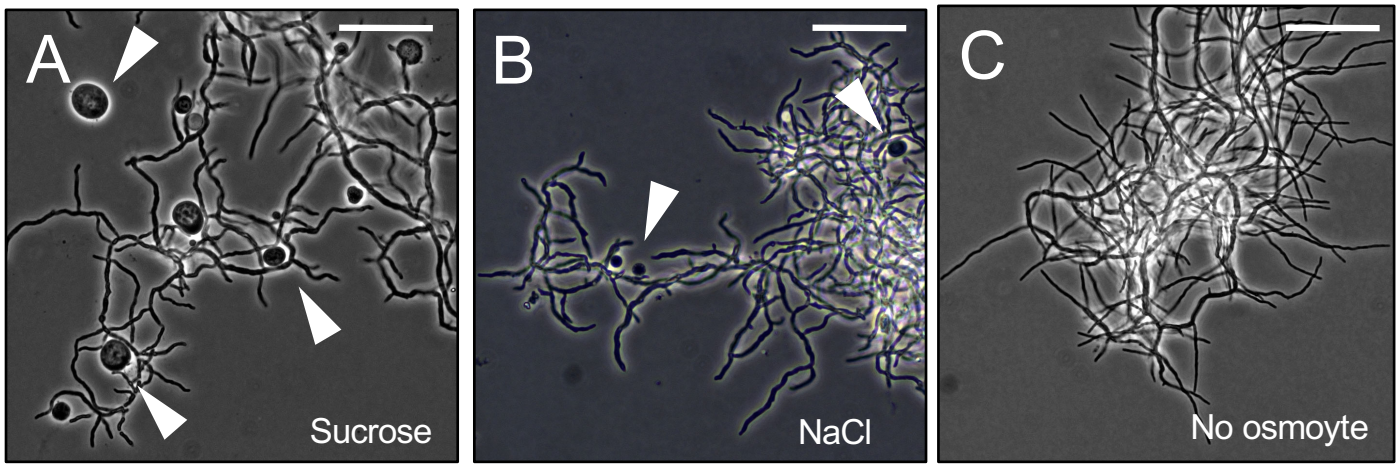

Extended Data Figure S1. Osmolytes are required for the formation of wall-less cells. The addition of 0.6M sucrose (A) or NaCl (B) to LPB medium is required for the formation of wall-less cells. No wall-less cells are detected without the addition of osmolytes (C). Scale bars represent 20 µm.

Extended Data Figure S1

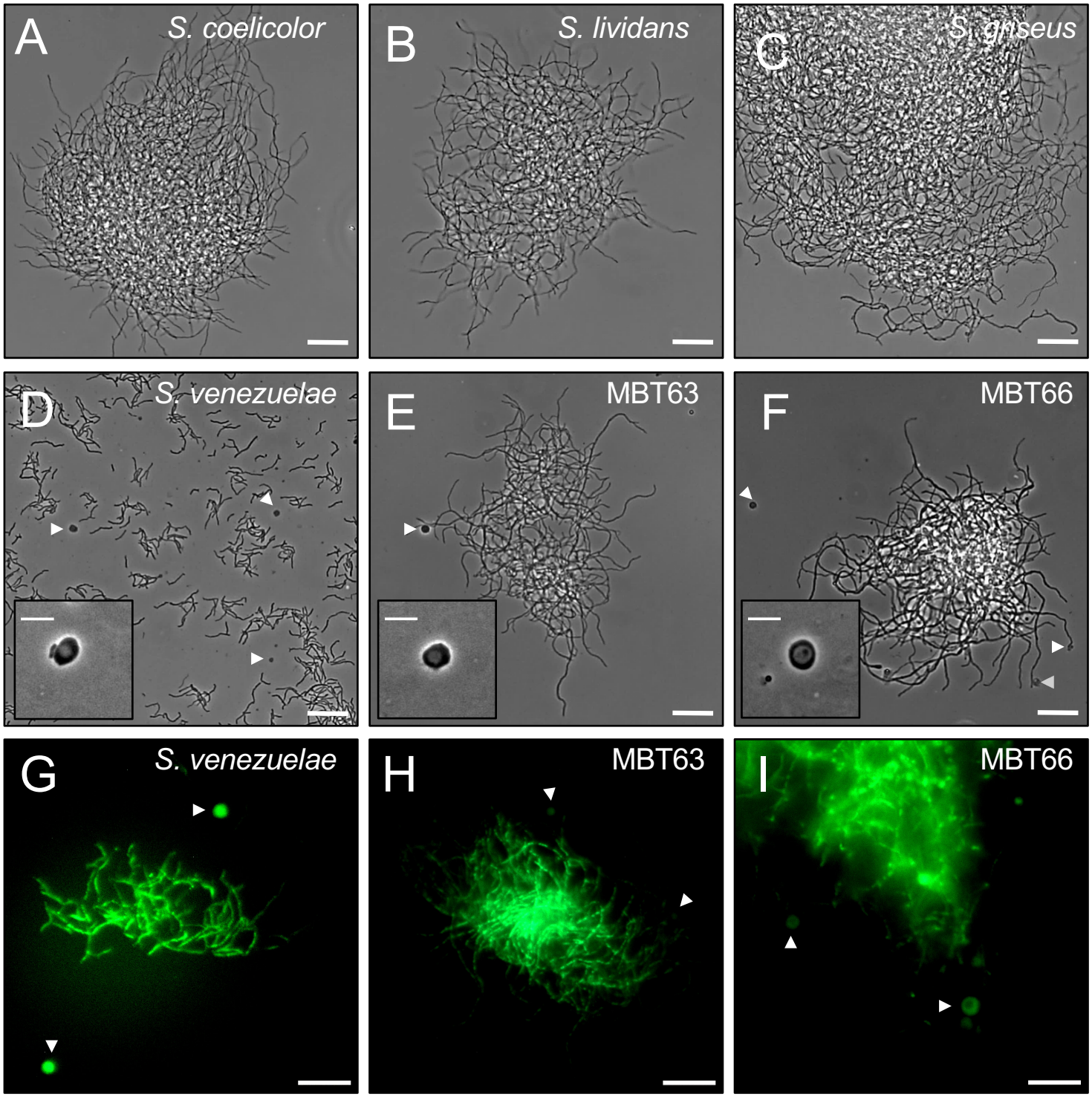

Extended Data Figure S2. Formation of wall-less cells in *Streptomyces* and *Kitasatospora* species. Unlike *Streptomyces coelicolor* (A), *Streptomyces lividans* (B) and *Streptomyces griseus* (C), wall-less (arrowheads) are evident in *Streptomyces venezuelae* (D), and *Kitasatospora* strains MBT63 (E) and MBT66 (F) grown in LPB medium. The inlays show magnified versions of wall-less cells in these species. (G-I). Visualization of DNA in wall-less cells using SYTO9. Scale bars represent 5 µm (inlays), 10 µm (G-I) or 20 µm (A-F).

Extended Data Figure S2

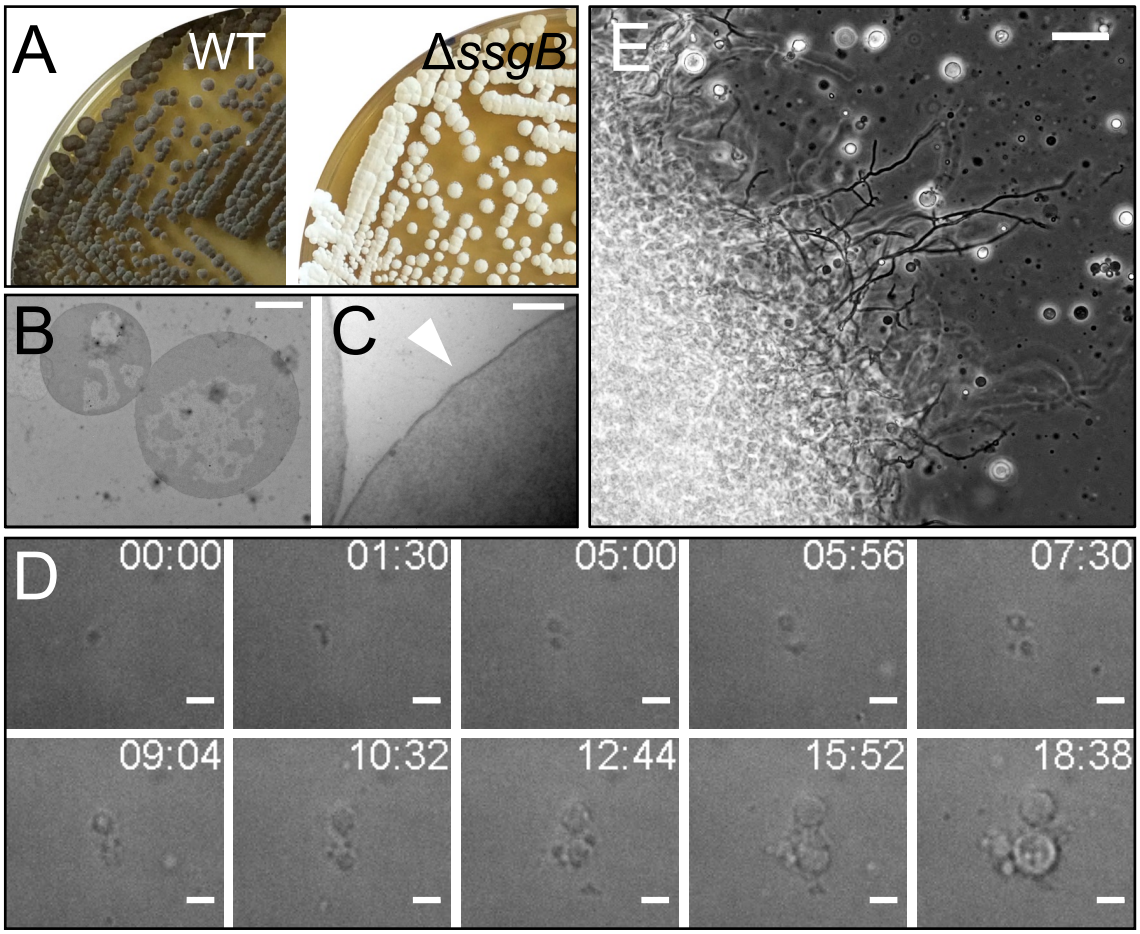

Extended Data Figure S3. Reversible metamorphosis in the *K. viridifaciens* Δ*ssgB* mutant. (A) Deletion of *ssgB* in *K. viridifaciens* blocks the formation of grey spores. (B, C) Transmission electron micrographs of N-forms of the Δ*ssgB* mutant strain indicates that they lack the cell wall. The arrowhead indicates the cell membrane (C). (D) Phase-contrast images from Extended Data Video S5 showing N-form proliferation in liquid medium. The times are indicated in HH:MM. (E) Plating of N-forms of the *ssgB* mutant on LPMA yields colonies consisting of mycelia and N-forms. Scale bars represent 200 nm (C), 2 µm (B), 10 µm (D) or 20 µm (E).

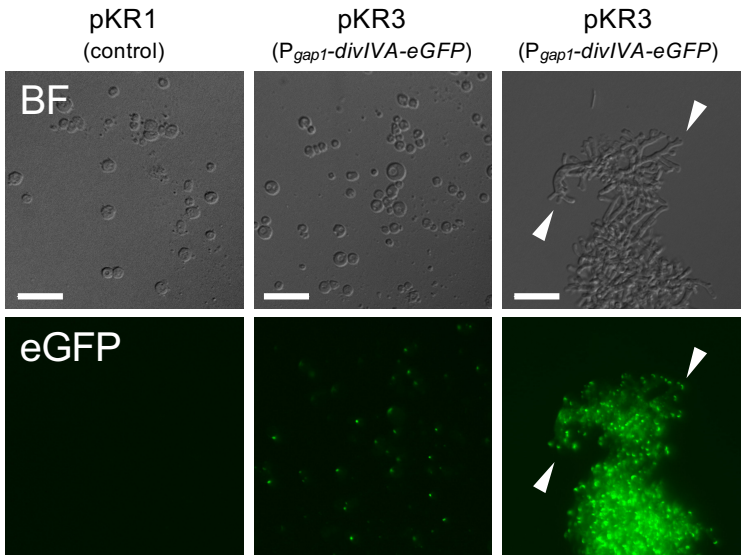

Extended Data Figure S4. Functional complementation of the Δ*divIVA* mutant by DivIVA-eGFP The DivIVA-eGFP fusion expressed from pKR3 restores filamentous growth of the *divIVA* mutant, and localizes to the hyphal tips (arrowheads). Scale bars represent 10 µm.

Extended Data Figure S4